



Biosynthesis of CuO Nanoparticles using *Coleus aromaticus* leaf Extract for Efficient Catalytic Applications

P. KALAIVANI¹ and G. MATHUBALA^{2*}

^{1,2*}Department of Chemistry, Bharath Institute of Higher Education and Research, BIST, Chennai-600073, India.

*Corresponding author E-mail: kalaivanipolur94@gmail.com

<http://dx.doi.org/10.13005/ojc/400514>

(Received: July 12, 2024; Accepted: October 17, 2024)

ABSTRACT

In today's world, the necessity to create economical and ecologically friendly processes has led to a huge increase in interest in the biosynthesis of CuO nanoparticles. Biosynthesis has been proposed as a route to developing various types of nanomaterials. This paper used a leaf extract of *Coleus aromaticus* as a reductant and stabilizing agent to employ a biosynthesis method to synthesize copper oxide nanoparticles. PXRD revealed the average particle size of the copper oxide nanoparticle is 30nm. The absorption peak at 564nm validated the UV-Vis spectra used to identify the production of copper oxide nanoparticles. The absorption peaks of the green synthesized CuO nanoparticles occur at 611 cm⁻¹, matching CuO stretching, indicating the formation of CuO nanoparticles. TGA was used to evaluate the material's thermal stability with CuO nanoparticles. Using SEM and TEM, the CuO nanoparticle's surface morphology, and spherical structure were investigated, and the copper oxide nanoparticles' average diameter was only 34.4nm. In addition, the obtained CuO nanoparticles were used as efficient catalysis for synthesizing diphenyl ether via the Ullmann coupling reaction. ¹H and ¹³C NMR spectroscopy, Fourier-transformed infrared spectroscopy analysis, and UV-Vis spectroscopy confirmed the produced diphenyl ether. The CuO nanoparticles synthesized using the *Coleus aromaticus* leaf extract technique produced a high yield of diphenyl ether. The outcomes demonstrated that leaf extract could synthesize copper oxide nanoparticles with high uniformity of particle sizes in a more environmentally friendly manner.

Keywords: Green synthesis, Plant defense, Catalyst, NMR, TGA.

INTRODUCTION

In recent decades, nanomaterial synthesis (like graphene, carbon nanotubes, metal nanoparticles, quantum dots, etc.) with dimensions between 10 and 100nm has drawn attention because of its potential uses in numerous sectors^{1,2}. CuO, along with a variety of transition metal oxides, is a

p-type semiconductor that has garnered significant attention due to its exceptional optical, magnetic, electrical, and physical properties³. In the fields of catalysis, electrochemistry, solar energy conversion, sensors/biosensors, energy storage, and biocide, CuO is widely used owing to its narrow band gap of 1.2 eV⁴. However, conventional methods of bulk synthesis require hazardous chemicals, even



though nanoparticles can be synthesized very rapidly⁵. There are several techniques available for preparing copper nanoparticles, including thermal reduction, capping agents, sonochemistry, metal vapor synthesis, microemulsion technologies, laser irradiation, and induced radiation⁶. Comparing this method with others such as chemical reduction, heat evaporation, electrochemical reduction, photochemical reduction, etc., the green synthesis approach was shown to be the best one⁷. To promote environmental sustainability, it has been emphasized to use green synthesis approaches that use mild reactions and non-hazardous precursors. In the green synthesis of NPs, bacteria, algae, and yeast are actively used, as well as plants and their derivatives (photosynthesis)⁸. Because the plant extract possesses reducing properties, this process involves capping and reducing copper nanoparticles by applying the leaf extract as a reducing and capping agent⁹. Since it was introduced more than 100 years ago, Ullmann-type aryl ether synthesis remains one of the most important tools for fine chemical synthesis on an industrial scale. Because of the importance of this research, significant efforts have been directed towards tailoring homogeneous copper catalysts¹⁰. The term "Ullmann condensation reaction," as used in commonly used nomenclature, describes a catalytic or stoichiometric copper interaction of an aryl halide with an amine, such as phenol, to create the appropriate aryl amine and ether molecules. in that order¹¹.

In response to the above discussions, we have synthesized CuO nanoparticles by a green synthesis method. Analyzing phase formation, surface morphologies, optical properties, and thermal properties of the prepared materials was carried out by various techniques. Additionally, diphenyl ether was synthesized through the Ullmann coupling reaction. Additionally, the obtained ether properties were characterized, confirming that diphenyl ether has been formed. Thus, green synthesis CuO nanoparticles are unique and exhibit excellent catalytic properties. Overall, there are additional benefits to this technology, such as the low catalyst loading, and rapid reaction times with large yields. FT-IR, ¹H NMR, ¹³C NMR, and UV-Visible spectroscopy were used to characterize them. Employing ecologically generated CuO nanoparticles as a potent catalyst to facilitate the bromobenzene-Ullmann reaction.

EXPERIMENTAL

Materials

We purchased ethanol and copper sulphate from Sigma-Aldrich. Fresh *Coleus aromaticus* leaves were collected from Polur, Tiruvannamalai District, Tamil Nadu. During the synthesis and washing process, deionized water was acquired from the Millipore plant.

Preparing the leaf extract of *Coleus aromaticus*

The *Coleus aromaticus* plant's leaves were gathered from Polur, Tiruvannamalai district, Tamil Nadu garden. The leaves were roughly chopped and then weighed. In 200 mL of double-distilled water, 50 g of finely chopped *Coleus aromaticus* leaves were added. The mixture was brought to a boil at 50°C for thirty minutes and stirred for two hours. It reached room T as it cooled. To obtain a clear solution, the extract was filtered through filter paper of Whatman No. 1. The filtrate solution was refrigerated at 4°C for future examination¹².

Green synthesis of CuO nanoparticles

A biosynthesis technique was used to create copper oxide nanoparticles. The synthesis procedure involves preparing a 100 mL standard flask with 1 mmol CuSO₄·5H₂O solution. In a 50 mL beaker, 30 mL of CuSO₄·5H₂O solution was added, and then 10 mL of leaf extract was added. For five hours, the reaction mixture was constantly stirred, after which it was left for twenty-four hours. Upon reduction of Cu²⁺, the transition from light to dark black color shows the development of copper oxide nanoparticles. Afterward, the product was cleaned using 100% C₂H₅OH and deionized water. The resulting CuO nanoparticles were then dried for ten hours at 60°C¹³. It is shown in Figure 1.

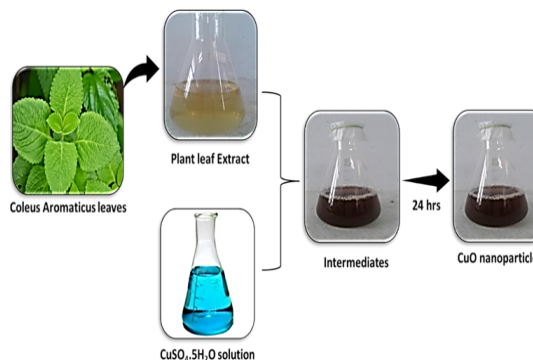


Fig. 1. CuO nanoparticle manufacturing process: color changes during the reduction of CuSO₄·5H₂O to CuO nanoparticles from *Coleus aromaticus* leaf extract

Materials characterization

CuO nanoparticle phase formation and crystal structure were investigated by powder XRD using a 2.2 KW Cu anode in a ceramic X-ray tube (Bruker, D8 Advance). The prepared material's molecular structure and functional groups were determined by FT-IR analysis using a Perkin Elmer RX-1. Utilizing scanning electron microscopy, the material's morphology and microstructure were identified using JEOL JSM 5600. Thermogravimetric analysis using TGA PerkinElmer SII (Diamond Series) examined the phase transformation and stability of the materials. The NMR instrumentation technique is beneficial for synthetic organic materials using 400 MHz (Bruker). UV-Vis Spectrophotometer using JASCO (V-670 PC). HR-TEM using FEI-Tecna G2 20 Twin.

RESULTS AND DISCUSSION

Structural studies

The size of the crystallite, phase identity, and nature of the crystalline synthesized materials can all be ascertained by PXRD. The XRD data of the CuO nanoparticles are displayed in Fig. 2. The peaks of diffraction in the prepared CuO are found at 10.8°, 27.7°, 29.3°, 31.7°, 32.8°, 48°, 52.8°, and 59.4°, corresponding to the planes (002), (100), (101), (102), (103), (006), (110), (108) and (116) of monoclinic structure. This agrees with previous literature, corroborating JCPDS card No. 77-1898¹⁴. The absence of additional diffraction peaks from other phases suggests that copper oxide nanoparticles are a pure phase. Applying the Debye-Scherrer formula, the principal peak of the sample's average crystalline size was determined¹⁵.

$$D = \frac{0.9 \lambda}{\beta \cos \theta}$$

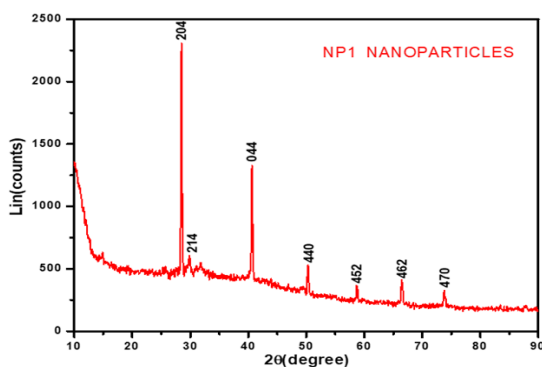


Fig. 2. XRD spectra of green synthesized CuO nanoparticles using *Coleus aromaticus* leaf extract

Calculated the average particle size for the CuO nanoparticles displayed in Table 1 using the aforementioned methodology. It is found that green synthesized CuO nanoparticles of 30nm in the average particle size. The results confirm the formation of CuO nanoparticles dispersed in leaf extracts of *Coleus aromaticus*¹⁶.

Table 1: Particle size of CuO nanoparticles using *Coleus aromaticus* leaf extract by Debye Scherrer formula

2θ (deg)	FWHM (β) radians	Particle Size (D) nm	d spacing	Plane hkl	Microstrain
29.71	0.2665	30	3.0045	214	0.0176

Functional group studies

As shown in Fig. 3(a and b), FT-IR spectroscopy investigated the synthesized materials' functional groups in the 500-4000 cm⁻¹ range. The absorption peaks of the CuO nanoparticles occur at 611 cm⁻¹, matching CuO stretching, indicating the formation of CuO nanoparticles. *Coleus aromaticus* leaf extract and as-prepared CuO nanoparticles have similar characteristic peaks, observed at 1090 and 1095 cm⁻¹, matching C-O stretching.

Furthermore, the stretching and bending vibrations of C=C are responsible for the 1639 and 1624 cm⁻¹ peaks in *Coleus aromaticus* leaf extract and as-prepared CuO nanoparticles. C-H bond stretching and bending vibrations are represented by the observed peaks in the 2922 and 2935 cm⁻¹ peaks in *Coleus aromaticus* leaf extract and as-prepared CuO nanoparticles. Furthermore, in the 3435 and 3402 cm⁻¹ regions, the peaks are caused by the OH stretching of water molecules¹⁷ in peaks in *Coleus aromaticus* leaf extract and prepared CuO nanoparticles.

UV-Vis analysis

The generated CuO nanoparticles' optical properties and *Coleus aromaticus* leaf extract were examined using UV-Vis. An absorption spectrum measurement is shown in Fig. 4(a and b). Considering the π-π* transition, the absorbance spectra of CuO nanoparticles were detected at 235, 239, 360, 364, and 392nm. An important absorption peak was observed at 401 and 404nm due to the n-π* transition. In addition, it was proven that CuO nanoparticles had formed by the absorption peak at 564nm. This is the most effective method of analysis to detect CuO nanoparticle Surface plasmon resonance¹⁸. It is shown in Figure 4(a and b).

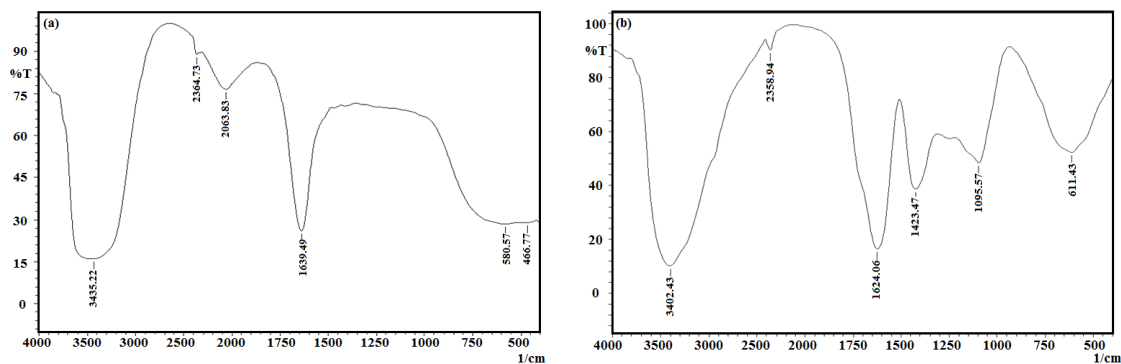


Fig. 3(a-b). FTIR spectra of a) leaf extract of *Coleus aromaticus*; b) green synthesized CuO nanoparticles using *Coleus aromaticus* leaf extract

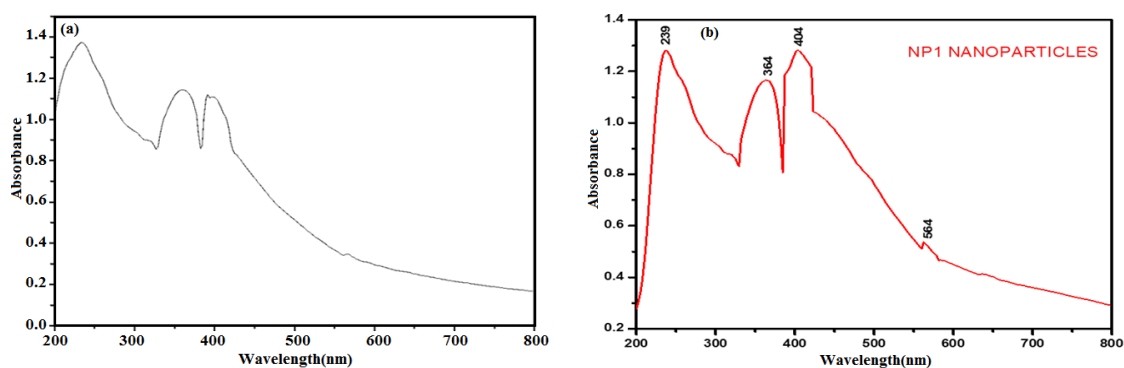


Fig. 4(a-b). UV-Vis spectra of a) leaf extract of *Coleus aromaticus* and b) green synthesized CuO nanoparticles using *Coleus aromaticus* leaf extract

Morphological studies

Scanning electron microscopy studies

Using scanning electron microscopy, the microstructure and surface morphology of CuO nanoparticles were examined. Fig. 5(a) and (b) reveal morphological information about CuO nanoparticles. The spherical shape of the agglomeration nanoparticles formed sphere-

like structure morphologies was observed¹⁹. HRSEM was used to analyze the copper oxide nanoparticles' topography, size, and morphology. Extremely polydisperse nanoparticles were present. Agglomerated copper oxide nanoparticles comprised many of the available samples. As a result, the SEM image verified the green synthesis of copper oxide nanoparticles' characteristics.

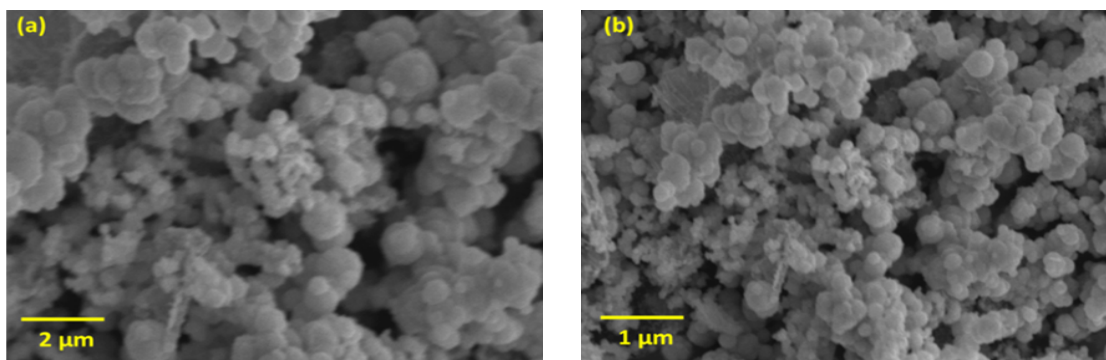


Fig. 5 (a-b). Scanning electron microscopy of green synthesized CuO nanoparticles using *Coleus aromaticus* leaf extract

HR-TEM studies

Furthermore, the CuO nanoparticle's internal structure was confirmed by TEM analysis,

as depicted in Fig. 6(a) and (b). The obtained morphologies show sphere-like morphologies, which corroborated with SEM results²⁰.

The spheres result from combustion, which raises temperatures to extremely high levels. The heat emitted during burning and the ensuing gas production are just a few of the many factors that could have contributed to the agglomeration, along with magnetic

interactions, low density, and weak interparticle forces. Image J was utilized to ascertain the HRTEM image's particle sizes' distribution frequency shown in Fig. 7. According to Fig. 6 (a), the copper oxide nanoparticles' average diameter was only 34.4nm.

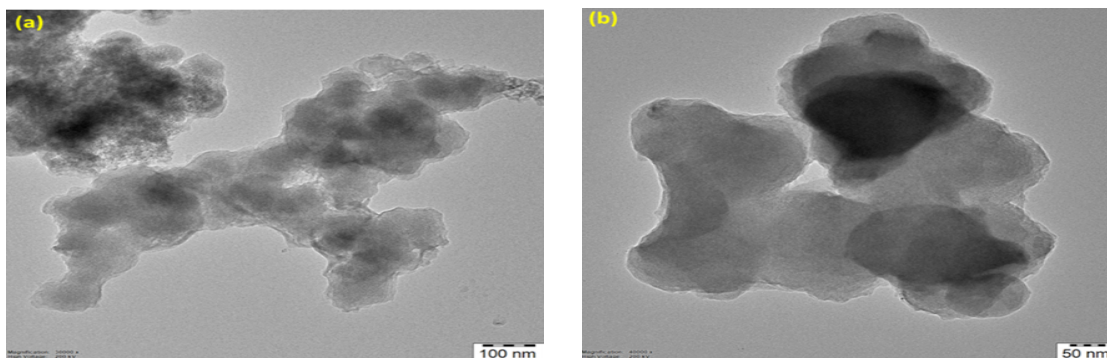


Fig. 6(a-b). HR-TEM image of green synthesized CuO nanoparticles using *Coleus aromaticus* leaf extract

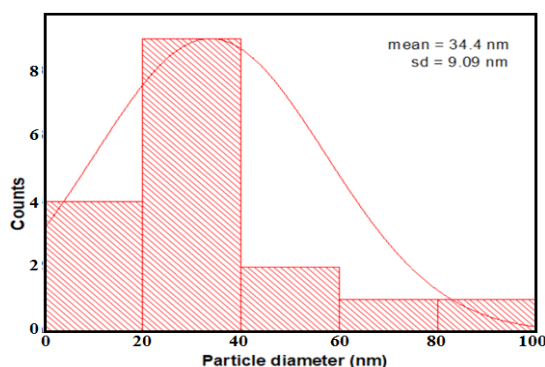


Fig. 7. Particle size distribution

TGA studies

TGA was utilized to evaluate the CuO nanoparticles' thermal stability at ambient temperatures up to 800°C. Fig. 8 depicts the TGA profile of CuO nanoparticles. Three steps of decomposition were observed from the TGA curve of CuO nanoparticles. The removal of water molecules and moisture is responsible for the initial weight loss (9%), which occurs below 166°C. The gradual weight loss was observed from 166°C up to 600°C due to the removal of organic solvent from CuO nanoparticles. Furthermore, abrupt weight loss was noted at 600°C because of the removal of CO, CO₂, and other organic gases following the pyrolysis and burning of organic molecules. As a result, no significant weight loss was observed at higher temperatures, which indicated the formation of high-purity copper oxide nanoparticles²¹.

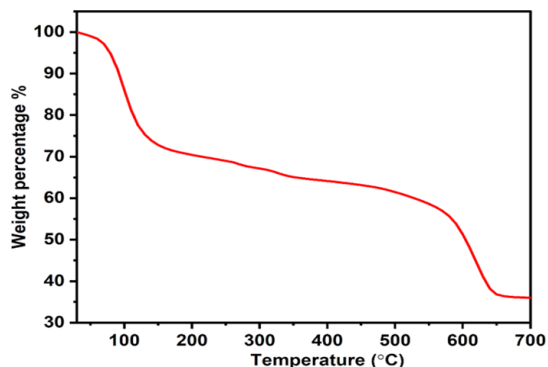


Fig. 8. Thermal gravimetric analyses of CuO nanoparticles using *Coleus aromaticus* leaf extract

Catalytic Applications

Procedure for synthesis of diphenyl ether:

In this work, the leaf extract of *Coleus aromaticus* was used to create catalyst copper oxide nanoparticles. The catalytic reactions were conducted with bromobenzene (2 mmol), KOH (2.0 equiv), and DMSO (2 mmol), stirred, and the

0.02 mmol of catalyst CuO nanoparticles were added to the reaction mixture. The reaction was performed for 30 min at 80°C in an ultrasonic bath for two hours. After the reaction, the suspension was collected and centrifuged. Thin layer chromatography monitored the reaction progress²². After being utilized in the procedure, the mixture cooled to room temperature. 10 mL of $\text{CH}_3\text{COOC}_2\text{H}_5$ was added to the resultant solution after the catalyst was isolated using simple filtration. Water was used to wash the organic layer, and anhydrous Na_2SO_4 was used to dry it. The crude product was produced via vacuum-assisted solvent evaporation. Hexane was used as the eluent in column chromatography to purify this, which created the desired result: yellow oil. UV, FTIR, ^1H , and ^{13}C NMR spectral studies were utilized to characterize the purified products. Ullmann coupling reaction using CuO nanoparticles as an efficient bromobenzene catalyst to obtain a diphenyl ether. The reaction mechanism is given in Figure 9.

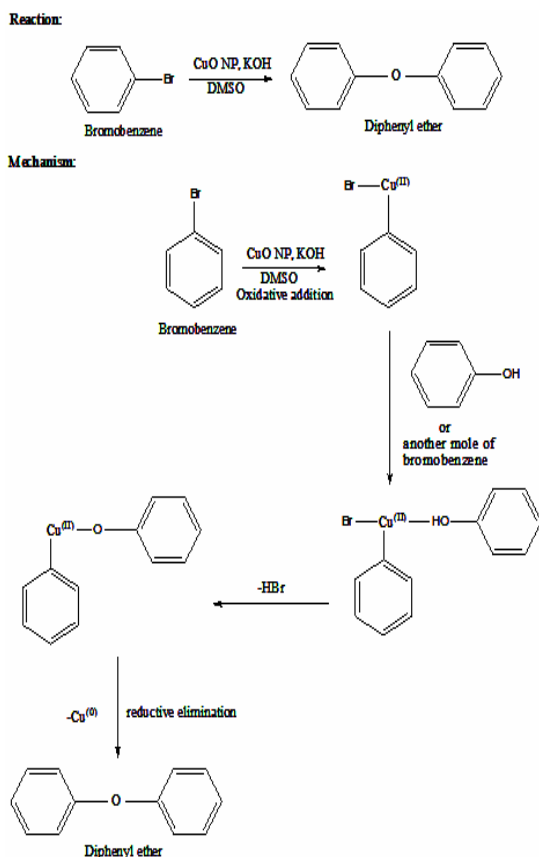


Fig. 9. Reaction and mechanism for Ullmann coupling reaction

In the first step, Cu(II) bromide reacts with a nucleophile in place of a KOH to allow acid removal. This process results in a complex between Cu and a nucleophile. The aryl bromide is then oxidized to the catalyst surface by accommodating aryl and bromide functionalities and oxidizing copper(I) to copper(0). Cu(0) is undergoing reductive elimination to form diphenyl ether and regenerates the catalyst (Cu-Br) for usage in the next catalytic cycle.

UV-Visible spectroscopy of diphenyl ether

The electronic spectrum of diphenyl ether synthesized using CuO nanoparticles shows a peak of absorption at 261 nm²³. This peak corresponds to the distinctive aromatic ring peak. The absorption peaks at 296 and 338 nm show the well-known C-O-C linkage peak. Both absorption peaks confirmed the formation of diphenyl ether, as shown in Figure 10(a).

FT-IR Spectroscopy

A helpful technique for figuring out a molecule's functional group is Fourier-transformed infrared spectroscopy. The signal at 3074 cm^{-1} was produced by stretching the aromatic C-H bond vibrations. OH, stretching vibrations peak at 3454 cm^{-1} . C=C stretching vibrations caused the sharp peak recorded at 1641, 1577, and 1471 cm^{-1} . The peak, which was measured at 1319, 1068, and 1014 cm^{-1} , was seen to exhibit stretching vibrations of C-O-C. The peak was caused by Cu-O stretching vibrations²⁴ and appeared at 677 and 459 cm^{-1} . It is shown in Figure 10(b).

NMR Spectroscopy

The signals corresponding to the synthesized compounds' protons were confirmed using ^1H NMR analysis using their chemical shifts, multiplicities, and coupling constants.

The protons on an aromatic ring should typically provide NMR signals in the H region between 6 and 8 ppm. When the proton in diphenyl ether is replaced with a functional group atom, the remaining aryl protons' chemical environment is altered²⁵.

^1H NMR spectrum of diphenyl ether^{26,27} (CDCl_3 , 400 MHz) δ ppm: 7.34-7.37 (t, 2H), 7.40-7.44 (m, 4H), 7.66-7.68 (d, 4H). It is shown in Fig. 10(c). ^{13}C NMR (400 MHz, CDCl_3 , ppm): δ 122.2-133.3. It is shown in Figure 10(d).

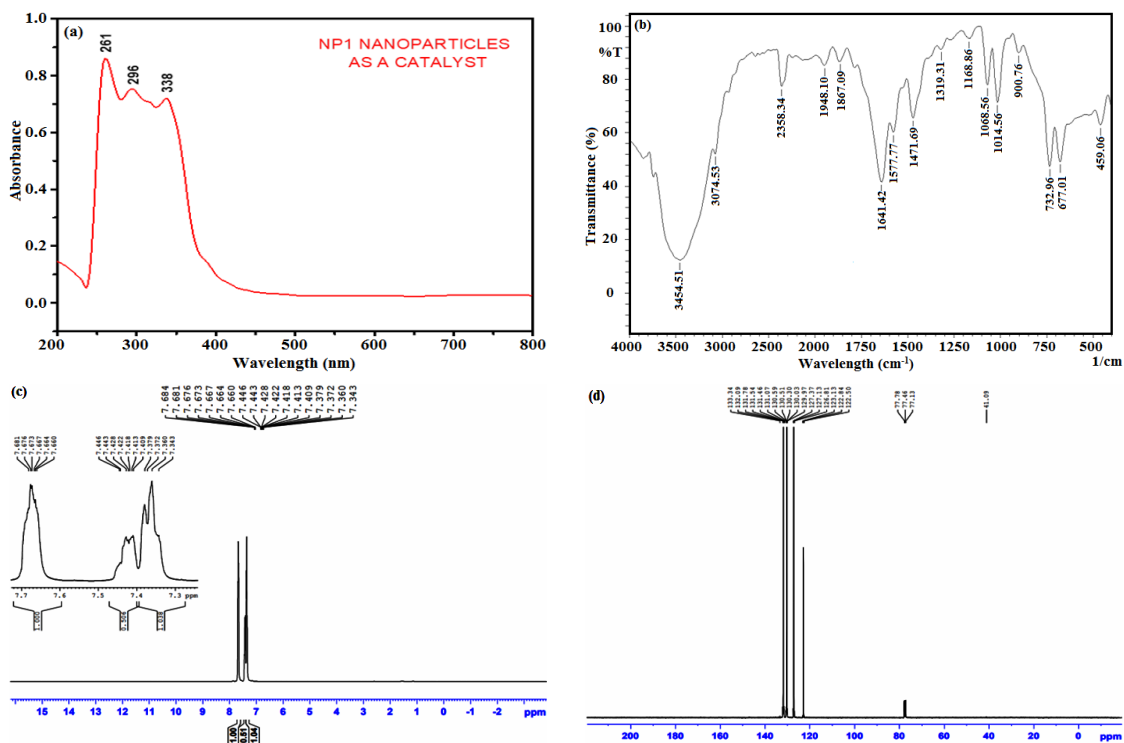


Fig. 10(a-d). Spectral studies of diphenyl ether using copper oxide nanoparticles from *Coleus aromaticus* as a catalyst (a) UV-Vis spectra (b) FT-IR spectra (c) ^1H NMR spectra, (d) ^{13}C NMR spectra

CONCLUSION

The green synthesis process used *Coleus aromaticus* leaf extract to produce the copper oxide nanoparticles successfully. The XRD analysis revealed the copper oxide nanoparticles formed a well-crystallite monoclinic structure, and the average crystal size of CuONP is approximately 30nm. SEM and TEM verified the sphere shapes and had a size range of 34.4nm of the synthesized copper oxide nanoparticles. The UV-Vis spectrum shows the increase in absorbance towards the higher wavelength side, indicating the role of leaf extract, and the wavelength is 564nm. Thermogravimetric analysis was used to determine the CuO nanoparticles' thermal stability in the material. The CuO stretching vibration peak at 611 cm^{-1} confirmed the copper oxide nanoparticle formation by FT-IR analysis. They were subjected to catalytic studies. Using copper oxide (NP1) nanoparticles as a catalyst to create diphenyl ethers was a unique, simple, and affordable process. The expected product is

yellowish oil. Diphenyl ether synthesis produced a 91% yield and was quite impressive. The products were analyzed by ^1H NMR, ^{13}C NMR, FT-IR, and UV-Visible analyses. A high yield of diaryl ether was produced by the *Coleus aromaticus* leaf extract method's CuO nanoparticles. Overall, there are many benefits to this technology, including low catalyst loading, and rapid reaction times with large yields in quick reaction times.

ACKNOWLEDGMENT

This research did not receive any specific grant from funding agencies in the public, commercial, or not-for-profit sectors.

Funding source

There was no funding source for this work.

Conflicts of interest

There are no financial conflicts of interest, according to the authors.

REFERENCES

1. Al-Douri Y.; Graphene, Nanotubes and Quantum Dots-Based Nanotechnology: Fundamentals and Applications., Woodhead Pub-Techn & Engineering., 2022.

2. Fritea L.; Banica F.; Costea TO.; Moldovan L.; Dobjanschi L.; Muresan M.; Cavalu S., Metal nanoparticles and carbon-based nanomaterials for improved performances of electrochemical (Bio) sensors with biomedical applications., *Materials.*, **2021**, *14*(21), 6319.
3. Chaudhary YS.; Agrawal A.; Shrivastav R.; Satsangi VR.; Dass S., A study on the photoelectrochemical properties of copper oxide thin films., *International Journal of Hydrogen Energy.*, **2004**, *29*(2), 131-4.
4. Wang Y.; Lany S.; Ghanbaja J.; Fagot-Revurat Y.; Chen YP.; Soldera F.; Horwat D.; Mücklich F.; Pierson JF., Electronic structures of Cu₂O, Cu₄O₃, and CuO: A joint experimental and theoretical study., *Phy Rev B.*, **2016**, *94*(24), 245418.
5. Denkba EB.; Celik E.; Erdal E.; Kavaz D.; Akbal Ö.; Kara G.; Bayram C., Magnetically based nanocarriers in drug delivery., *Nanobio. Drug. Delv.*, **2016**, 285-331.
6. Usman MS.; Zowalaty ME.; Shameli K.; Zainuddin N.; Salama M.; Ibrahim NA., Synthesis, characterization, and antimicrobial properties of copper nanoparticles., *Inter. Jour. Nanomed.*, **2013**, 4467-79.
7. Geoprincy G.; Sri BV.; Poonguzhali U.; Gandhi NN.; Renganathan S., A review on green synthesis of silver nanoparticles., *Asian Jour. Pharm and Clinical Res.*, **2013**, *6*(1), 8-12.
8. Khan F.; Shahid A.; Zhu H.; Wang N.; Javed MR.; Ahmad N.; Xu J.; Alam MA.; Mehmood MA., Prospects of algae-based green synthesis of nanoparticles for environmental applications., *Chemosphere.*, **2022**, *293*, 133571.
9. Antonio-Pérez A.; Durán-Armenta LF.; Pérez-Loredo MG.; Torres-Huerta AL., Biosynthesis of copper nanoparticles with medicinal plants extracts: from extraction methods to applications., *Micromachines.*, **2023**, *14*(10), 1882.
10. Hassan J.; Sévignon M.; Gozzi C.; Schulz E.; Lemaire M., Aryl-aryl bond formation one century after the discovery of the Ullmann reaction., *Chem. Rev.*, **2002**, *102*(5), 1359-470.
11. Sperotto E.; Van Klink GP.; Van Koten G.; De Vries JG., The mechanism of the modified Ullmann reaction., *Dalton Trans.*, **2010**, *39*(43), 10338-51.
12. Subaiea G.; Alafnan A.; Alamri A.; Hussain T.; Hassoun SM.; Lila AS.; Khafagy ES.; Katamesh AA., Coleus aromaticus Ethanolic Leaves Extract Mediates Inhibition of NF- B Signaling Pathway in Lung Adenocarcinoma A549 Cells., *Processes.*, **2023**, *11*(5), 1332.
13. Chalandar HE.; Ghorbani HR.; Attar H.; Alavi SA., Antifungal effect of copper and copper oxide nanoparticles against Penicillium on orange fruit., *Biosci. Biotech. Res Asia.*, **2017**, *14*(1), 279-84.
14. Roguai S.; Djelloul A., A simple synthesis of CuO NPs for photocatalytic applications and their structural and optical properties., *Journal of New. Tech and Mat.*, **2021**, *11*(2), 53-7.
15. Zakirov MI.; Semen'Ko MP.; Korotchenkov OA., A simple sonochemical synthesis of nanosized ZnO from zinc acetate and sodium hydroxide., *Jour. Nano and Electr. Physics.*, **2018**, *10*(5), 05023.
16. Kolahalam LA.; Prasad KR.; Krishna PM.; Supraja N.; Shanmugan S., The exploration of bio-inspired copper oxide nanoparticles: synthesis, characterization and *in-vitro* biological investigations., *Heliyon.*, **2022**, *8*(6), 09726.
17. Dodoo-Arhin D.; Leoni M.; Scardi P., Microemulsion synthesis of copper oxide nanorod-like structures., *Mole. Cryst and Liq. Crystals.*, **2012**, *555*(1), 17-31.
18. Prathap N.; Dravid N.; Kaarmukhilnilavan SR.; Shivakumar MS.; Venkatesan S.; Shaik MR, Shaik B., Copper Oxide Nanoparticles Synthesized from Indigofera linnaei Ali and This Plant's Biological Applications., *Inorganics.*, **2023**, *11*(12), 462.
19. Reddy KR., Green synthesis, morphological and optical studies of CuO nanoparticles., *Journ. Mole. Structure.*, **2017**, *1150*, 553-7.
20. Murthy HA.; Zeleke TD.; Tan KB.; Ghotekar S.; Alam MW.; Balachandran R.; Chan KY.; Sanaulla PF.; Kumar MA.; Ravikumar CR., Enhanced multifunctionality of CuO nanoparticles synthesized using aqueous leaf extract of Vernonia amygdalina plant., *Res. Chem.*, **2021**, *3*, 100141.
21. Mali SM.; Narwade SS.; Navale YH.; Tayade SB.; Digraskar RV.; Patil VB.; Kumbhar AS.; Sathe BR., Heterostructural CuO–ZnO nanocomposites: a highly selective chemical and electrochemical NO₂ sensor., *ACS Omega.*, **2019**, *4*(23), 20129-41.

22. Robotjazi ZS.; Naimi-Jamal MR.; Tajbakhsh M., Synthesis and characterization of highly efficient and recoverable Cu@ MCM-41-(2-hydroxy-3-propoxypropyl) metformin mesoporous catalyst and its uses in Ullmann type reactions., *Scientific Reports.*, **2022**, *12*(1), 4949.
23. Kumar Y.; Singh V.; Pandey A.; Genwa M.; Meena PL., Synthesis, characterization and antibacterial activity of ZnO nanoparticles., *InAIP Conference Proceedings.*, **2020**, *1*, 2265, AIP Publishing.
24. Javid-Naderi MJ.; Sabouri Z.; Jalili A.; Zarrinfar H.; Samarghandian S.; Darroudi M., Green synthesis of copper oxide nanoparticles using okra (*Abelmoschus esculentus*) fruit extract and assessment of their cytotoxicity and photocatalytic applications., *Envir. Tech & Innovation.*, **2023**, *32*, 103300.
25. Liu F.; Wei Z.; Wang L.; Wang Z., Synthesis, experimental and theoretical investigation of molecular structure, IR, Raman spectra and ¹H NMR analyses of 4, 4 -dihydroxydiphenyl ether and 4, 4 -oxybis (1-methoxybenzene)., *Journal of Molecular Structure.*, **2013**, *1035*, 285-94.
26. Buck E.; Song ZJ.; Tschaen D.; Dormer PG.; Volante RP.; Reider PJ., Ullmann diaryl ether synthesis: Rate acceleration by 2, 2, 6, 6-tetramethylheptane-3, 5-dione., *Organic letters.*, **2002**, *4*(9), 1623-6.
27. Karthik AD.; Geetha K., Ullmann Condensation Via O-Arylation of Phenol using Nano Copper Derived From Copper(II) Precursor., *International Journal of ChemTech Research.*, **2015**, *7*(3), 1578-1585.